Towards bimodal photonic sensing with coherent readout in silicon nitride

Student paper

Antonia Torres-Cubillo[1,*], J. Manuel Luque-González[1], Alejandro Sánchez-Postigo[1,3], J. Gonzalo Wangüemert-Pérez[1,2], Íñigo Molina-Fernández[1,2] and Robert Halir[1,2]

[1]Telecommunication Research Institute (TELMA), Universidad de Málaga, Louis Pasteur 35, 29010 Málaga, Spain
[2]IBIMA-BIONAND, Parque Tecnológico de Andalucía, 29590 Málaga, Spain
[3]Currently at Institute of Physics, University of Münster, Heisenbergstraße 11, 48149 Münster, Germany
[*] atc@ic.uma.es

Photonic integrated sensors have emerged as an attractive tool for medical diagnosis and environmental monitoring, offering quantitative results in real time. In this work, we develop and experimentally validate a novel silicon nitride bimodal interferometric sensor with a coherent phase retrieval. This approach has potential to combine the compactness and relaxed temperature sensitivity of bimodal sensors with the linear and unambiguous phase readout of coherent detection.
Keywords: *Integrated photonics, bimodal waveguide, refractive index sensor, coherent readout*

INTRODUCTION

Photonic integrated sensors have attracted a lot of research interest over the past decade [1], as they can be used to perform label-free chemical analysis and deliver quantitative results in real time. In fact, several sensing configurations have been proposed to detect analytes such as pathogens [2] and hazardous gasses [3], which is critical in medical diagnosis and environmental monitoring. Furthermore, silicon-based sensors are compatible with standard CMOS fabrication processes and can potentially be mass-produced, encouraging the development of new concepts like lab-on-a-chip devices and distributed sensor networks.

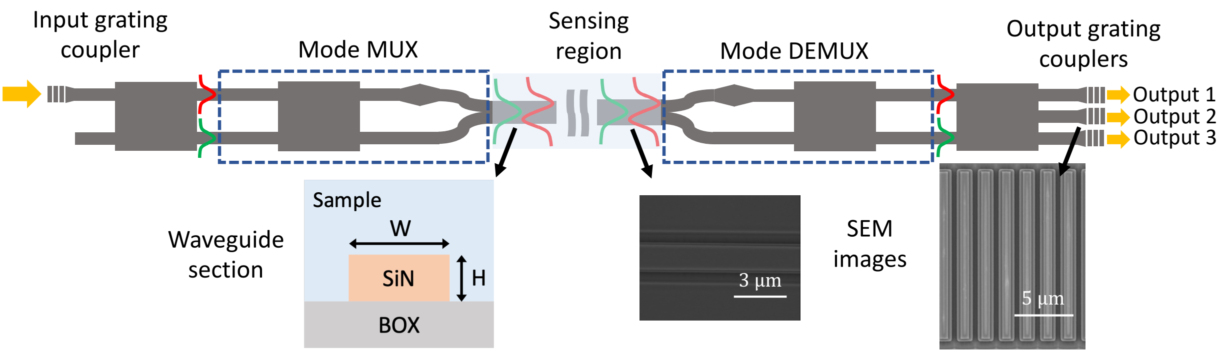

Fig. 1. Schematic representation of the bimodal refractive index sensor. Input light is split by a 2×2 MMI and used to excite the first two TE modes of the bimodal sensing waveguide. A sensing window is etched to enable sample-light interaction. After propagating through the waveguide, the two modes are demultiplexed and enter a 2×3 MMI, which provides three 120° outputs, ready for the coherent phase readout.

Among the different sensing configurations, interferometric sensors offer fixed-wavelength operation and can be extremely sensitive: Mach Zehnder interferometers combined with a 120° 2×3 hybrid enable coherent phase detection [4], overcoming limitations like directional ambiguity and sensitivity fading, and yielding remarkable detection limits [5]. However, this configuration requires both a sensing and a reference arm and is sensitive to temperature fluctuations. Bimodal sensors emerge as an interesting alternative [6, 7]: two different modes propagate through the same waveguide, but with different sensitivities to the surroundings, thus creating an interference pattern at the output when the refractive index of the sample changes. This differential interferometry not only reduces the footprint of the sensor, but also increases its robustness, as both modes will be affected by the same temperature changes in the waveguide.

In this work, we present a silicon nitride interferometric sensor, which combines a bimodal sensing waveguide with a coherent phase readout and the use of calibration algorithms [see Fig. 1], validated with preliminary sensing experiments.

WORKING PRINCIPLE

A schematic representation of the proposed refractive index sensor is shown in Fig. 1. The sample circulates through a microfluidic channel which will be placed on top of the sensing region. A sensing window is opened over this area to enable an overlap between the sample and the evanescent field of the guided modes. A change in the concentration of the analyte in the sample induces a proportional change of its refractive index (Δn_c), which is translated by the waveguide into a change in the effective index of each mode ($\Delta n_{\mathrm{eff},1}, \Delta n_{\mathrm{eff},2}$). In a bimodal waveguide, the fundamental mode is more confined than the second-order mode and its effective index will change at a smaller rate. We define the differential sensitivity of the waveguide as

$$S_\mathrm{d} = \frac{\partial n_{\mathrm{eff},2}}{\partial n_\mathrm{c}} - \frac{\partial n_{\mathrm{eff},1}}{\partial n_\mathrm{c}}. \quad (1)$$

Our interferometric sensing architecture transforms the index change in the cladding into three readily detectable output signals. For that purpose, fixed-wavelength laser light is split into the two single-mode inputs of a mode multiplexer [8] used to excite the first-order and second-order modes of the sensing bimodal waveguide. Due to the interaction with the sample, after propagating through the waveguide, the two modes have accumulated a relative phase shift $\Phi = S_\mathrm{a} S_\mathrm{d} \Delta n_\mathrm{c}$, where

$$S_\mathrm{a} = \frac{2\pi}{\lambda_0} L \quad (2)$$

is the sensitivity of the architecture, λ_0 is the vacuum wavelength and L is the length of the sensing waveguide. The two modes are demultiplexed into two fundamental modes, which enter the 120° hybrid**.** This device delivers three interferometric output signals, with a phase shift of 120° between them. These signals can be detected with photodetectors and combined to generate an IQ signal with phase Φ. Deterministic hardware errors can be corrected with different calibration algorithms [4, 9]. Once the phase is read, the change in analyte concentration can be immediately inferred.

SENSOR DESIGN

Our sensors have been designed for the Cornerstone silicon nitride platform [10]. This platform offers a 300 nm device layer and a 3 μm BOX thickness. The 2 μm silicon dioxide cladding is removed over the sensing region to enable light-matter interaction. The operation wavelength is 1520 nm and the employed polarization is TE. The three main components of our sensors are the bimodal sensing waveguide, the mode multiplexer and the 120° hybrid.

Simulations using FIMMWAVE mode solver software [11] were carried out to design the sensing waveguide, which is 1.8 μm wide and supports the two first TE modes. To evaluate its differential sensitivity, the change in the effective index of the guided modes was calculated as a function of a change in the refractive index of the cladding around a value of 1.32 RIU, which corresponds to pure water at the operating wavelength. The second TE mode is significantly more sensitive to changes in the cladding than the fundamental one, yielding a differential sensitivity of $S_\mathrm{d} = 0.08\ \mathrm{RIU/RIU}$, from which we get a system sensitivity of $S_\mathrm{a} \cdot S_\mathrm{d} = 1.72 \cdot 10^3\ \mathrm{rad/RIU}$, for a waveguide length of $L = 5.2\ \mathrm{mm}$. The mode converter and multiplexer comprises a 2×2 MMI, a 90° phase-shifter and a sinusoidal profile Y-branch, as shown in Fig. 1. The operational principles of this architecture are explained in detail in [12]. The 2×2 MMI has a width of 7.4 μm and a length of 127 μm, the phase shifter is 25.5 μm in length with a maximum width of 1.1 μm and the Y-branch is 30 μm long. The 2×3 MMI section of the 120° hybrid is 13.3 μm wide and 264 μm long. Light input and output is carried out by grating couplers, which are positioned with a pitch of 127 μm to enable the use of a fiber array polished at 26° as a cost-effective way to detect several simultaneous outputs.

EXPERIMENTAL RESULTS

A simple experimental setup consisting of a laser source operating at a fixed wavelength, an angled-polished fiber array, three photodetectors, alignment stations and a data acquisition module was arranged to validate our sensors. An isopropanol droplet, with a refractive index of 1.35 RIU, was carefully deposited on top of the sensing window. The evaporation of the sample caused a monotonic change of the refractive index of the cladding, thus inducing a proportional phase shift between the fundamental and the second TE modes of the bimodal waveguide. This phase shift was retrieved from the three output signals of the sensor, from which a fragment is shown in Fig. 2(a). We were able to correct the effect of hardware errors such as the observed power imbalances between the outputs by means of a simple ellipse-to-circle blind calibration algorithm [4], delivering a precise phase readout, represented in Fig. 2(b).

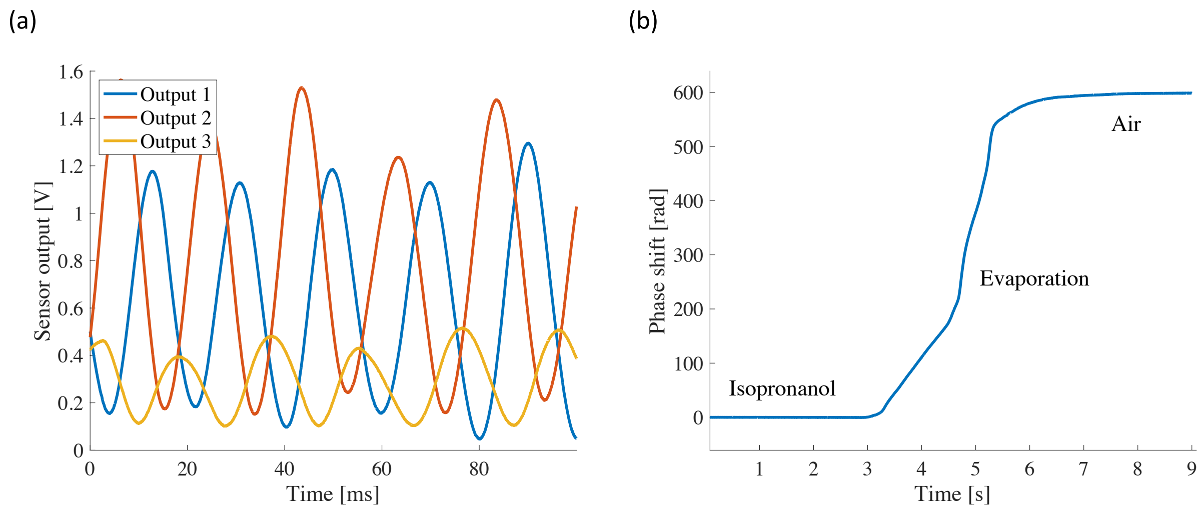

Fig. 2. (a) Sensor output signals. The evaporation of an isopropanol droplet causes a monotonic change in the refractive index of the cladding, resulting in three 120° shifted interferometric signals. (b) Phase readout. The retrieved phase enables the calculation of the sensitivity of the system.

We observed a phase shift of 600 rad from the deposition of the isopropanol droplet ($\mathrm{RI} = 1.35\,\mathrm{RIU}$) to its complete evaporation, leaving only air ($\mathrm{RI} = 1\,\mathrm{RIU}$) on the waveguide. The calculated systemic sensitivity is $S_\mathrm{a} \cdot S_\mathrm{d} = 600/(1.35-1) = 1.71 \cdot 10^3\ \mathrm{rad/RIU}$, which matches the theoretical value. These results are promising and encourage further experiments towards the detection of clinically relevant analytes.

CONCLUSIONS

We have developed a sensing configuration combining a bimodal interferometer with a coherent phase readout, facilitated by a simple architecture to perform the modal MUX/DEMUX. Our sensors have been fabricated on a silicon nitride platform and have been experimentally validated by simple sensing experiments, yielding promising results. Further work will involve a sophisticated microfluidics system to enable a controlled interaction with the sample for a precise sensor characterization and the detection of complex chemical substances. We consider that this is a significant step towards a robust, compact and cost-effective label-free sensing device.

Acknowledgements: This work has received funding from the Ministerio de Universidades, Ciencia e Innovación (FPU19/03330) and the Junta de Andalucía (Agencia Andaluza del Conocimiento PY18-793). We would also like to acknowledge the Universidad de Málaga.

References

[1] N. L. Kazanskly et at., *Advancement in silicon integrated photonics technologies for sensing applications in near-infrared and mid-infrared region: A review*, MDPI Photonics, vol. 9, no. 5, 2022.
[2] J. Maldonado et al., *Label-free detection of nasocomial bacteria using a nanophotonic interferometric biosensor*, Analyst, vol. 145, 2020.
[3] M. Vlk et al., *Extraordinary evanescent field confinement waveguide sensor for mid-infrared trace gas spectroscopy*, Light: Science and Applications, vol. 10, no. 26, 2021.
[4] R. Halir et al., *Direct and sensitive phase readout for integrated waveguide sensors*, IEEE Photonics Journal, vol. 5, no. 4, 2013.
[5] J. Leuermann et al., *Coherent silicon photonics interferometric sensor with an inexpensive laser source for sensitive label-free immunoassays*, Optics Letters, vol. 45, no. 24, 2020.
[6] L. Torrijos-Morán et al., *Integrated optical bimodal waveguide biosensors: Principles and applications*, Results in Optics, vol. 9, 2022.
[7] O. Calvo-Lozano et al., *One-step and real-time detection of microRNA-21 in human samples for lung cancer biosensing diagnosis*, Analytical Chemistry, vol. 94, no. 42, pp. 14659-14665, 2022.
[8] D. González-Andrade et al., *Experimental demonstration of a broadband mode converter and multiplexer based on subwavelength grating waveguides*, Optics and Laser Technology, vol. 129, 2020.
[9] P. Reyes-Iglesias et al., *High-performance monolithically integrated 120° with relaxed hardware constraints*, Optics Express, vol. 20, no. 5, 2012.
[10] https://www.cornerstone.sotonfab.co.uk
[11] https://www.photond.com
[12] D. González-Andrade et al., *Ultra-broadband mode converter and multiplexer based on sub-wavelength structures*, IEEE Photonics Journal, vol. 10, no. 2, pp. 2201010, 2018.